

USING NON-SMOOTH MULTI-DOMAIN DYNAMICS TO IMPROVE THE SAFETY ON HAUL ROADS IN SURFACE MINING

K. Thoeni¹, M. Servin² and A. Giacomini¹

¹ Centre for Geotechnical Science and Engineering
The University of Newcastle
Callaghan, NSW 2308, Australia
<http://www.newcastle.edu.au>

² UMIT Research Lab
Umeå University
Umeå, SE-90187, Sweden
<http://www.umu.se>

Key words: NDEM, MBD, Haul Truck, Granular Material, Collision

Abstract. The paper presents a preliminary numerical study aimed to improve the safety on haul roads in surface mining. The interaction and collision between granular berms and ultra-class haul trucks are investigated by using non-smooth multi-domain dynamics. The haul truck is modelled as a rigid multibody system and the granular berm as a distribution of rigid particles using the discrete element method. A non-smooth dynamics approach is applied to enable stable and time-efficient simulation of the full system with strong coupling. The numerical model is first calibrated using full-scale data from experimental tests and then applied to investigate the collision between the haul truck and granular berms of different geometry under various approach conditions.

1 INTRODUCTION

Berms of granular materials are commonly used along haul roads of surface mines to protect haul trucks from rolling over an edge and to avoid collisions. Their current design is based on rules of thumb [1]. However, their behaviour is still poorly understood and accidents, where haul trucks collide with a berm and run over the edge and down the front slope, are still happening on a regular basis [2]. In addition, there is common sense that the current rules of thumb do not apply to the new generation of ultra-class haul trucks but it is unclear how berms need to be designed in order to be efficient for stopping a runaway haul truck. Hence, the need for a more rigorous design approach is emerging within the mining industry and accurate specific numerical modelling could represent a valid tool for this purpose. The main aim of the current research is to understand, how

efficient granular berms are in stopping a runaway haul truck. Therefore, it is crucial to understand the behaviour of a granular berm upon collision with a haul truck travelling at various velocities. This problem is very complex and has to take into account large displacements of the granular material the berm is built of and the interaction of such material with large-scale mobile equipment. In addition, the variability of the available material on site used to build the berms, mostly waste rock material of various origins and grade, should also be considered [1]. Generally this material has a huge variation in terms of particle size, particle shape and hardness and cannot be easily characterised.

The *discrete element method* (DEM) is widely used to study the dynamic behaviour of granular materials including waste rock material. More recently, the DEM has also been coupled to *multibody dynamics* (MBD) for the investigation of soil–structure interaction problems and the simulation of the working process of construction machines [3, 4]. MBD allows studying the dynamic behaviour of interconnected rigid or flexible bodies, each of which can undergo large translational and rotational displacements. It is therefore the ideal method to model mobile equipment such as the haul truck. Coupled with the DEM it will allow to capture the dynamic behaviour of the machine and its interaction with granular material in an efficient way. Simulation coupling is, however, associated with a number of challenges that affect the computational performance, stability or interface forces between the coupled systems [5].

The following work presents an attempt to provide a deeper understanding of the problem using non-smooth multi-domain dynamics. The haul truck and the granular berm are modelled by means of a non-smooth approach to multibody dynamics and discrete elements that automatically support strong coupling without co-simulation. The general numerical framework is presented in Section 2 followed by a discussion on the calibration and validation (Section 3). Finally, preliminary results of simulations of collisions between a haul truck and granular berms of different berm geometry under various approach conditions are presented in Section 4.

2 NUMERICAL FRAMEWORK

The haul truck and the granular berm are modelled within the non-smooth multi-domain dynamics framework of the commercial software package AGX Dynamics [6]. In *non-smooth multi-domain dynamics*, the simulated system is composed by multiple heterogeneous subsystems with stiff dynamics and unanticipated events where the connectivity and number of variables suddenly change. The dynamics that occur on short time scales, compared to the time-step, are best treated as non-smooth [7, 8, 9]. This means that velocities may change discontinuously in accordance with some impact law, expressed in terms of inequality and complementarity conditions, in addition to the equations of motion and the differential algebraic equations used to describe the sub-systems. This is necessary for implicit time-stepping of dynamic systems with impacts, dry friction, joint limits, electric and hydraulic circuit switching that cause instantaneous impulse propagation throughout the system. The *non-smooth discrete element method* (NDEM)

implemented in AGX Dynamics can be seen as a time-implicit version of the classical smooth DEM [10]. The contact forces are modelled using impact laws and kinematic constraints for unilateral contacts and friction. Hence it allows strong dynamic coupling with other multibody systems such as the haul truck.

The equations of motion for modelling granular materials strongly coupled with rigid multibody systems are [11]:

$$\mathbf{M}\dot{\mathbf{v}} + \dot{\mathbf{M}}\mathbf{v} = \mathbf{f}_{\text{ext}} + \mathbf{G}_n^T \boldsymbol{\lambda}_n + \mathbf{G}_t^T \boldsymbol{\lambda}_t + \mathbf{G}_r^T \boldsymbol{\lambda}_r + \mathbf{G}_j^T \boldsymbol{\lambda}_j, \quad (1)$$

$$0 \leq \varepsilon_n \boldsymbol{\lambda}_n + \mathbf{g}_n + \tau_n \mathbf{G}_n \mathbf{v} \perp \boldsymbol{\lambda}_n \geq 0, \quad (2)$$

$$\gamma_t \boldsymbol{\lambda}_t + \mathbf{G}_t \mathbf{v} = 0, \quad |\boldsymbol{\lambda}_t^{(\alpha)}| \leq \mu_t |\mathbf{G}_n^{(\alpha)T} \boldsymbol{\lambda}_n^{(\alpha)}|, \quad (3)$$

$$\gamma_r \boldsymbol{\lambda}_r + \mathbf{G}_r \mathbf{v} = 0, \quad |\boldsymbol{\lambda}_r^{(\alpha)}| \leq \mu_r r |\mathbf{G}_n^{(\alpha)T} \boldsymbol{\lambda}_n^{(\alpha)}|, \quad (4)$$

$$\varepsilon_j \boldsymbol{\lambda}_j + \eta_j \mathbf{g}_j + \tau_j \mathbf{G}_j \mathbf{v} = 0. \quad (5)$$

Eq. (1) is the Newton-Euler equation of motion for rigid bodies with external (smooth) forces \mathbf{f}_{ext} and constraint force $\mathbf{G}^T \boldsymbol{\lambda}$ with Lagrange multiplier $\boldsymbol{\lambda}$ and Jacobian \mathbf{G} , divided into normal (n), tangential (t), rolling (r) and articulated and possibly motorised joints (j). \mathbf{M} is the generalised mass matrix and \mathbf{v} is the generalised velocity vector. Eqs. (2)-(3) are the Signorini-Coulomb conditions with constraint regularisation and stabilisation terms ε_n , τ_n and γ_t . With $\varepsilon_n = \tau_n = 0$, Eq. (2) states that bodies should be separated or have zero overlap, $\mathbf{g}_n(\mathbf{x}) \geq 0$, and if so the normal force should be non-cohesive, $\boldsymbol{\lambda}_n \geq 0$. With $\gamma_t = 0$, Eq. (3) states that contacts should have zero relative slide velocity, $\mathbf{G}_t \mathbf{v} = 0$, provided that the friction force remains bounded by the Coulomb friction law with friction coefficient μ_t . Eq. (4) similarly constrains relative rotation of contacting bodies provided the constraint torque do not exceed the rolling resistance law with rolling resistance coefficient μ_r and radius r . The constraint force, $\mathbf{G}_j^T \boldsymbol{\lambda}_j$, arise for articulated rigid bodies jointed with kinematic links and motors represented with the generic constraint of Eq. (5). With $\varepsilon_j, \tau_j = 0$ and $\eta_j = 1$, it becomes an ideal holonomic constraint $\mathbf{g}(\mathbf{x}) = 0$. For $\varepsilon, \eta = 0$ and $\tau = 1$, it becomes an ideal Pfaffian constraint $\mathbf{G}\dot{\mathbf{x}} = 0$. With $\varepsilon, \eta, \tau \neq 0$ it can represent a generic constraint with compliance and damping.

The Lagrange multiplier $\boldsymbol{\lambda}$ become an auxiliary variable to solve for in addition to position and velocity. The regularisation and stabilisation terms, ε and γ , introduce compliance and dissipation in motion orthogonal to the constraint manifold. The numerical time integration scheme is based on the SPOOK stepper [12] derived from discrete variational principle for the augmented system $(\mathbf{x}, \mathbf{v}, \boldsymbol{\lambda}, \dot{\boldsymbol{\lambda}})$ by applying a semi-implicit discretisation. Stepping the system position and velocity, $(\mathbf{x}_i, \mathbf{v}_i) \rightarrow (\mathbf{x}_{i+1}, \mathbf{v}_{i+1})$, from time t_i to $t_{i+1} = t_i + h$ involves solving a mixed complementarity problem [13]. This is solved using a hybrid solver where a projected Gauss-Seidel solver [10] is applied for the NDEM subsystem and a direct solver for the articulated rigid multibodies.

3 CALIBRATION AND VALIDATION

The experimental full-scale tests presented in [1] are used for calibration of the main input parameters and validation of the coupled model. In the experiments, a haul truck reversed into a trapezoidal granular berm and the motion of the truck was monitored using high-speed cameras. The granular material is modelled by spherical particles with a diameter in the range of 60 to 700 mm. The granular berm is initialised in a mould and friction is set to zero initially in order to get a dense granular assembly. The shape effect of the particles is taken into account using a rolling friction model. The haul truck considered in the following study is a CAT 797F. This is an ultra-class haul truck with a gross vehicle weight of 624 t (fully loaded). The load is not modelled explicitly, instead the mass of the empty body is adapted to reflect the gross vehicle weight. The centre of mass of the vehicle is positioned to reflect the manufacturer’s specifications (i.e., mass distribution front 34% and rear 66%). The key dimensions of the truck are summarised in Tab. 1. The MBD model of the truck is built from a simplified CAD model and comprises 19 rigid bodies. The suspension is explicitly modelled and the tyres are represented by a two-body tyre model [14].

Table 1: Key dimensions of the CAT 797F.

Description	Dimension
Overall rear tyre width	6.23 m
Overall length	15.08 m
Height (empty)	7.00 m
Wheelbase	7.19 m
Tyre diameter	4.02 m
Tyre width	1.47 m

A sensitivity analysis is performed to identify the most critical parameters. The analysis showed that the contact parameters (e.g., elasticity, friction, rolling) have a secondary influence on the results. The two main parameters influencing the results are the centre of mass of the vehicle and the geometry of the berm. The former is not known exactly and it is assumed according to the manufacturer’s specifications. The latter is crucial especially in the area where the truck first contacts the berm. In fact, the numerical model of the berm introduces a sharp kink between terrain and berm. In the experimental tests, the transition from terrain to berm is much smoother and the shape of the berm in the experiment is not a perfect trapezoid.

Fig. 1 shows a comparison between the measured results of one test presented in [1] and the numerical predictions using the final set of calibrated parameters. The numerical model is able to predict the general trend of the experimental test reasonably well, however, it can be noted that the predicted wheel climb and horizontal wheel displacement

are slightly lower. The numerical model gives almost identical results for both left hand side (LHS) and right hand side (RHS) whereas the experimental values vary considerably between the two wheels. This is justified by the ideal trapezoidal shape of the numerical berm compared to the rather irregular berm shape used in the experiment. Fig. 2 shows a comparison of a screenshot of the numerical simulation and an image from the experimental tests where this difference can clearly be seen.

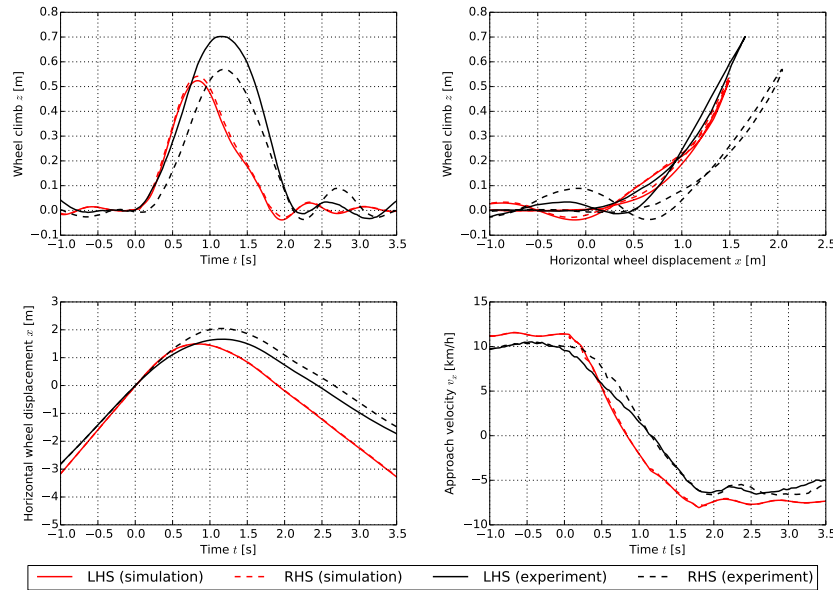


Figure 1: Measured vs. predicted results for final set of calibrated parameters.

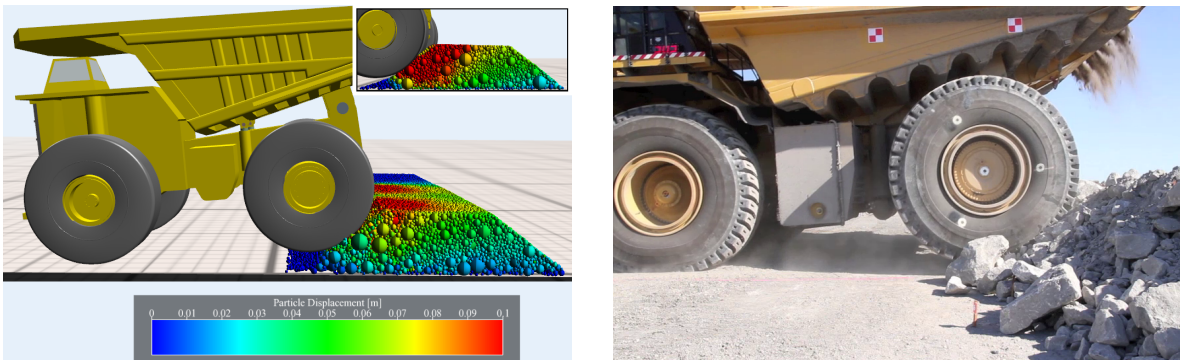


Figure 2: Screenshot of the numerical simulation (left) and corresponding picture from the experimental full-scale testing (right) at maximum wheel climb.

4 NUMERICAL INVESTIGATIONS

In the following, the numerical model is applied to investigate if the haul truck can be safely stopped by the granular berm. In particular, the study considers the collision between the haul truck and granular berms of different geometry under various approach conditions. Two main scenarios are considered. In the first scenario, the ultra-class haul truck is reversing into a triangular berm at relatively low velocity. This represents a dump-point scenario similar to the one investigated in [1]. The second scenario represents a runaway haul truck that is colliding head-on with a granular berm at higher velocities. Such a scenario is relevant for trapezoidal roadside berms and ramps where truck drivers could potentially lose control. In both cases, the length of the granular berm is 12 m and the truck is initialised with a specific velocity in the centre in front of the berm. The batter angle of the berms is 40° . The particle size distribution is the same as in Section 3.

Figs. 3–4 and Figs. 5–6 summarise the results for the first scenario where the haul truck is reversing with a velocity of $v = 15$ km/h and colliding with a triangular berm of height $H = 2$ m and $H = 3$ m respectively. From the horizontal wheel position in Fig. 3 it can clearly be seen that the rear axle passes the centreline of the berm with $H = 2$ m. Fig. 5 shows the same results for a berm with $H = 3$ m. In this case, the numerical model predicts that the rear axle of the truck is not passing the centreline. Hence, increasing the berm height from $H = 2$ m to $H = 3$ m provides safe stopping conditions and at the same time it keeps the truck back from the edge of a dump. It should be noted, that the maximum reversing speed of a CAT 797F ultra-class haul truck is $v = 11.9$ km/h. The considered reversing velocity is slightly higher in order to be on the safe side.

Figs. 7–8 and Figs. 9–10 summarise the results for the second scenario where the haul truck is colliding head-on with a trapezoidal granular berm with $H = 4$ m and a top width of $B = 1$ m and $B = 4$ m respectively. The truck is initialised with a velocity of $v = 40$ km/h (the actual top speed of a CAT 797F is $v = 67.6$ km/h). For the berm with $B = 1$ m the numerical model predicts that the front axle passes the end of the berm (Fig. 7). This could have fatal consequences considering that in most cases there would be a slope at the other side of the berm. Increasing the berm width from $B = 1$ m to $B = 4$ m provides safe stopping conditions (Fig. 9). This can also be seen when comparing the screenshots in Fig. 8 and Fig. 10.

5 CONCLUSIONS

In this paper, non-smooth multi-domain dynamics is used to investigate the collision between an ultra-class haul truck and granular berms used in surface mining. The haul truck is represented by rigid bodies interconnected with ideal joints and the granular material is modelled using rigid spherical particles. First, the numerical model is calibrated and validated using full scale experimental tests. Then the model is used to investigate two typical scenarios. In the first scenario the truck is reversing into a triangular berm. The effect of the berm height is shown. In the second scenario the truck is colliding

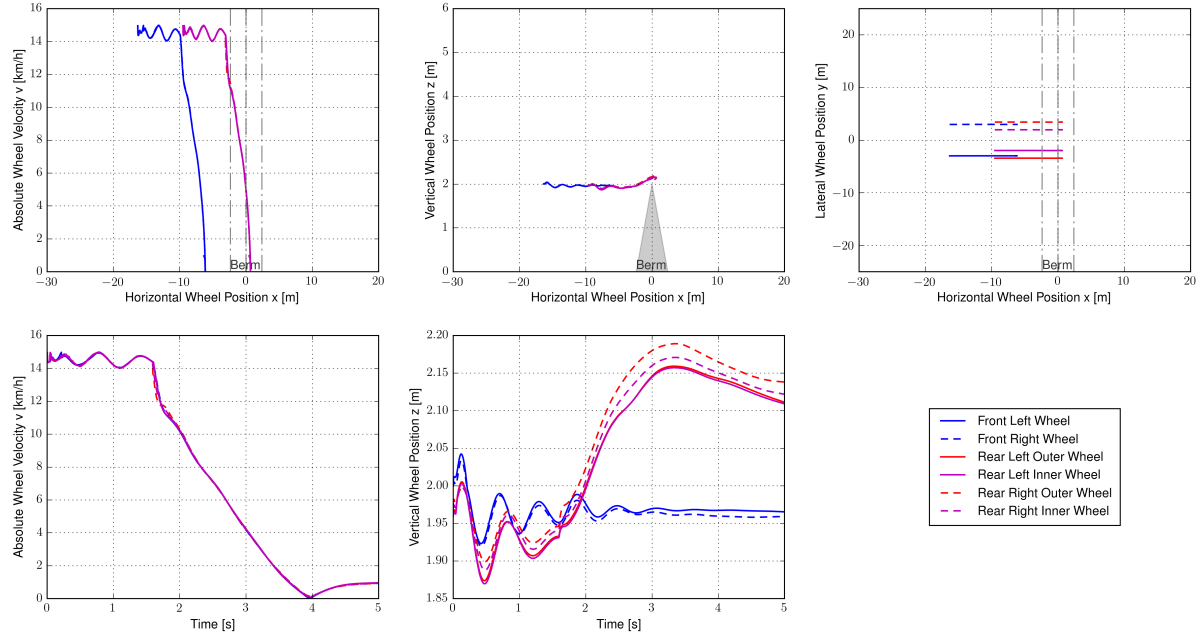


Figure 3: Summary of results for reversing scenario with $v = 15$ km/h and triangular berm with $H = 2$ m.

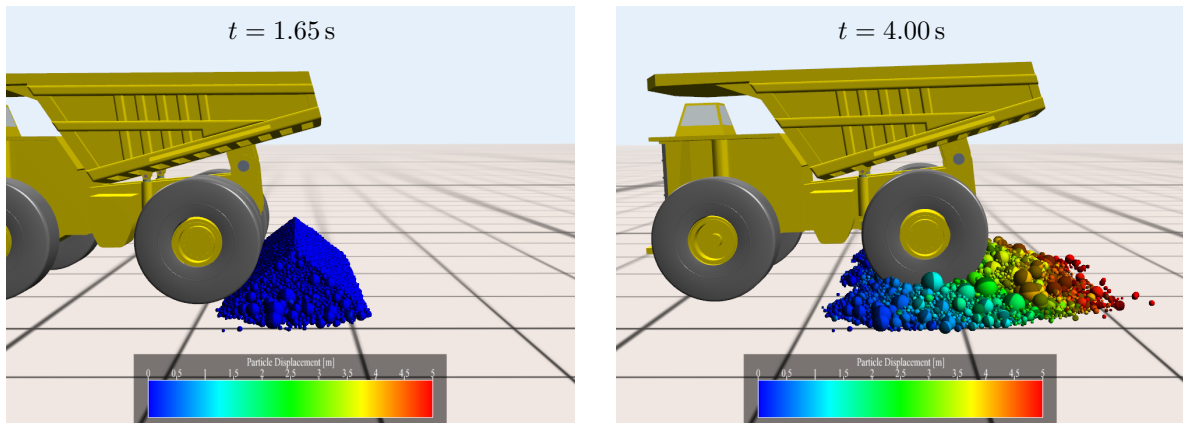


Figure 4: Screenshots of the collision at different time steps t for reversing scenario with $v = 15$ km/h and triangular berm with $H = 2$ m.

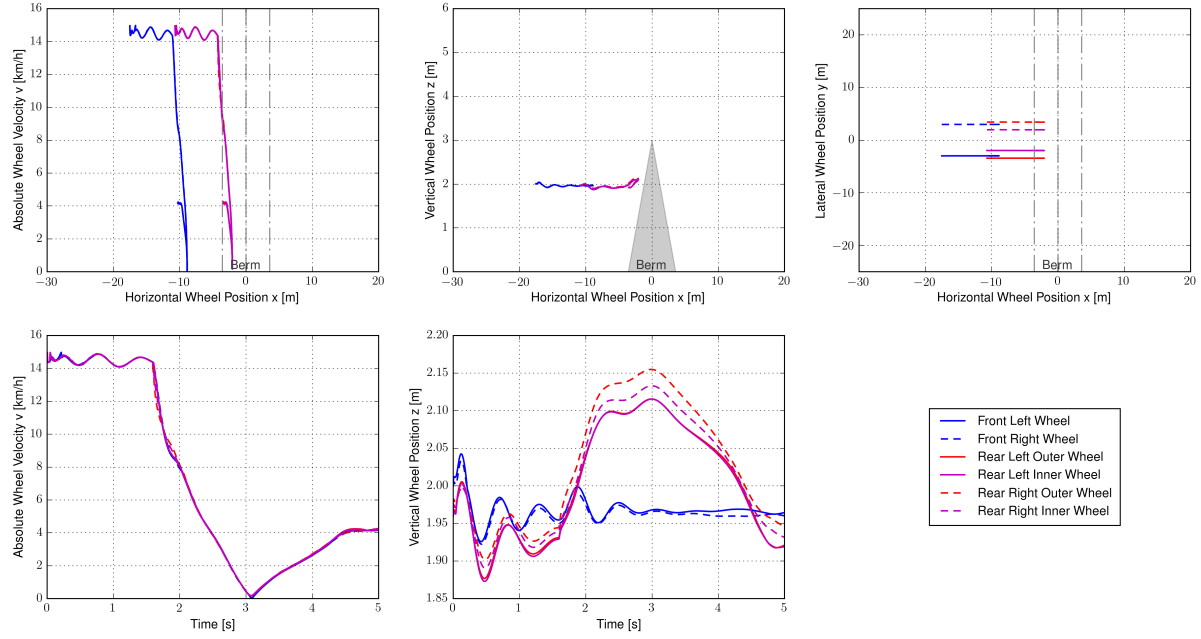


Figure 5: Summary of results for reversing scenario with $v = 15$ km/h and triangular berm with $H = 3$ m.

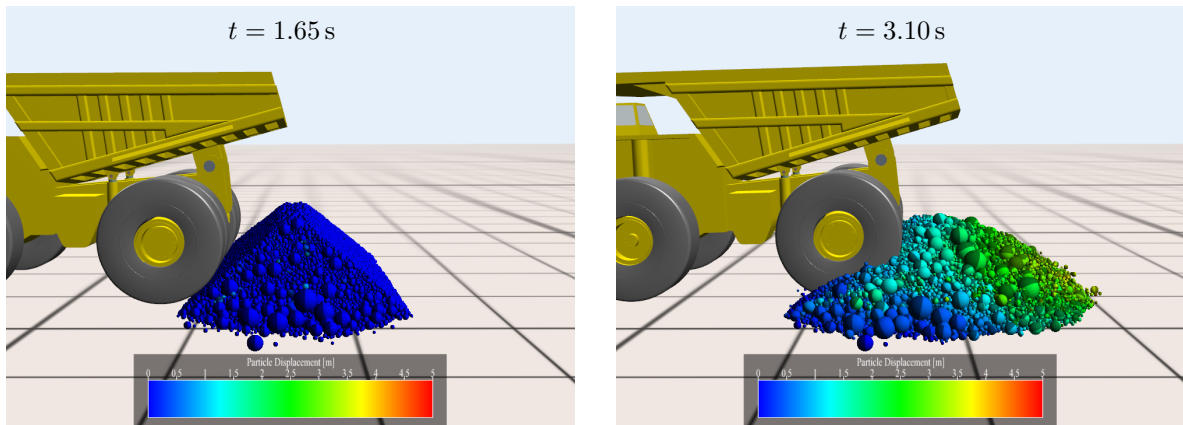


Figure 6: Screenshots of the collision at different time steps t for reversing scenario with $v = 15$ km/h and triangular berm with $H = 3$ m.

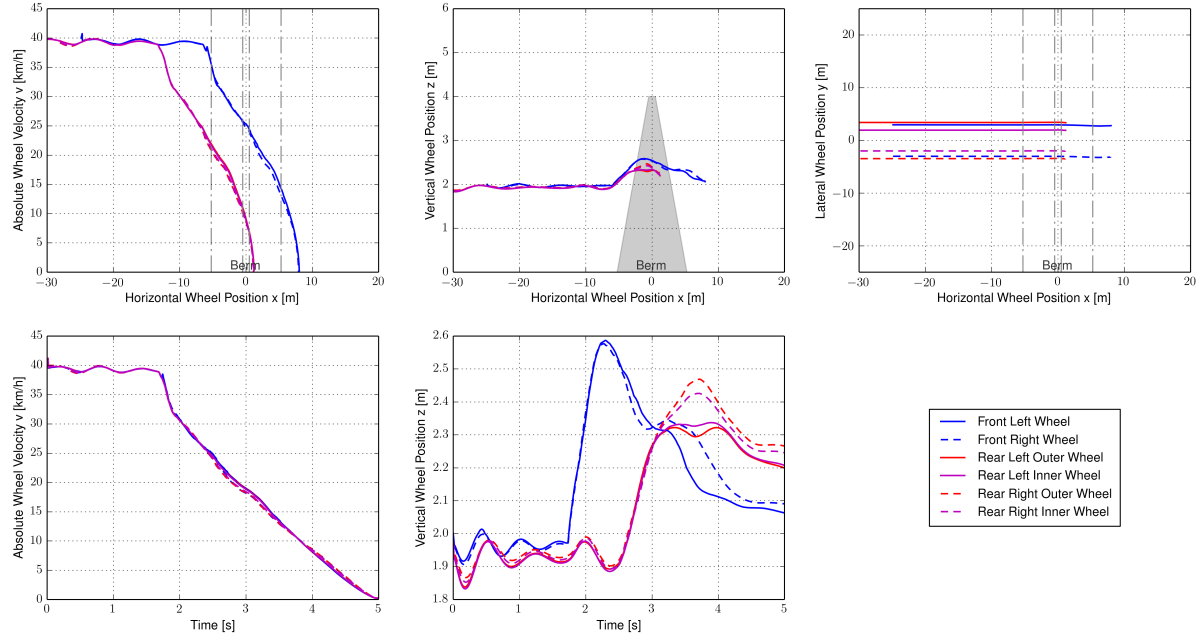


Figure 7: Summary of results for head-on collision with $v = 40$ km/h and trapezoidal berm with $H = 4$ m and $B = 1$ m.

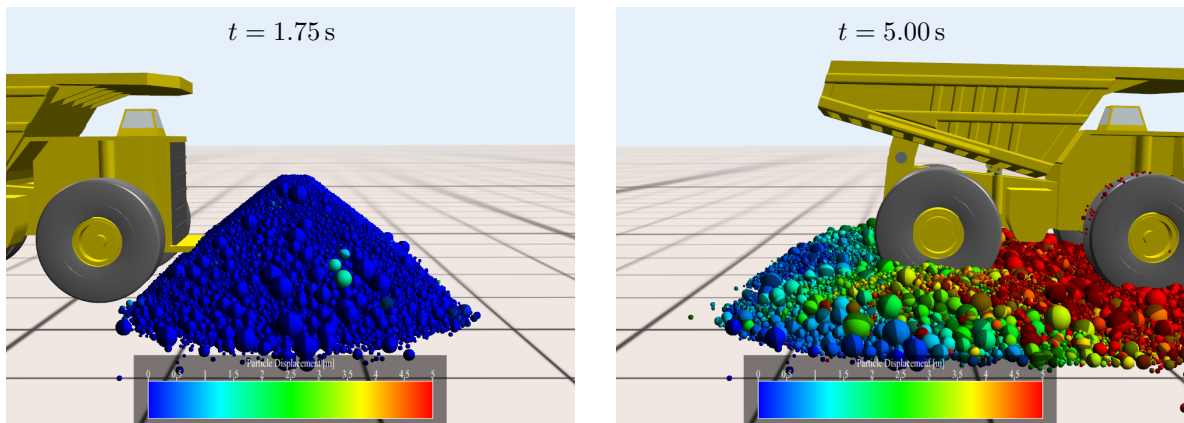


Figure 8: Screenshots of the collision at different time steps t for head-on collision with $v = 40$ km/h and trapezoidal berm with $H = 4$ m and $B = 1$ m.

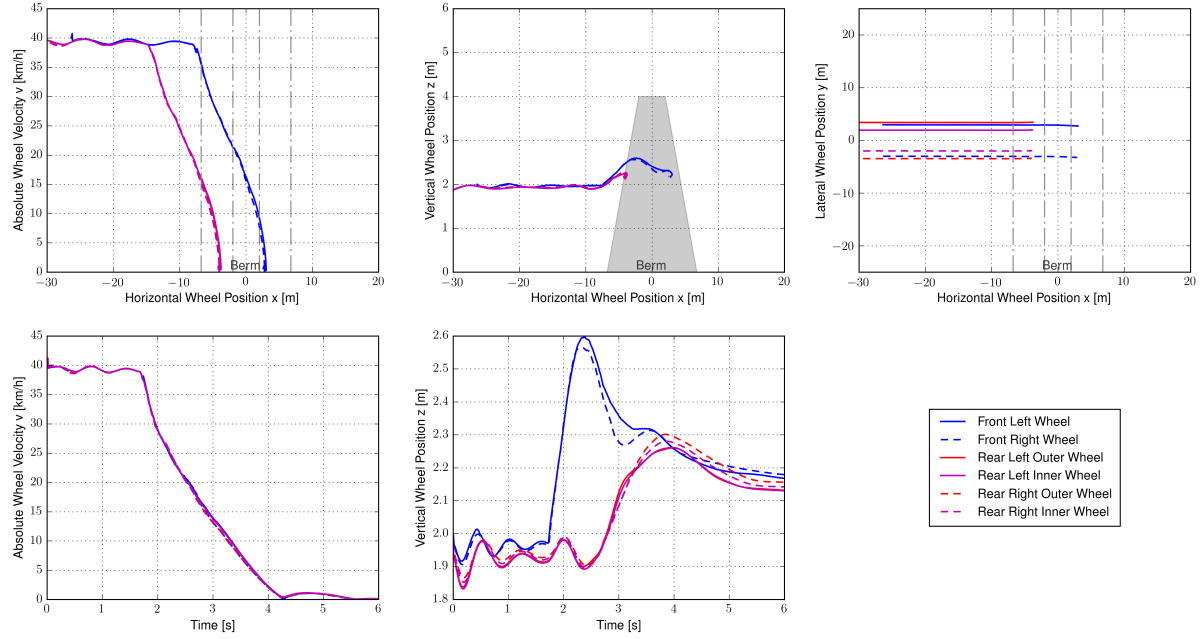


Figure 9: Summary of results for head-on collision with $v = 40$ km/h and trapezoidal berm with $H = 4$ m and $B = 4$ m.

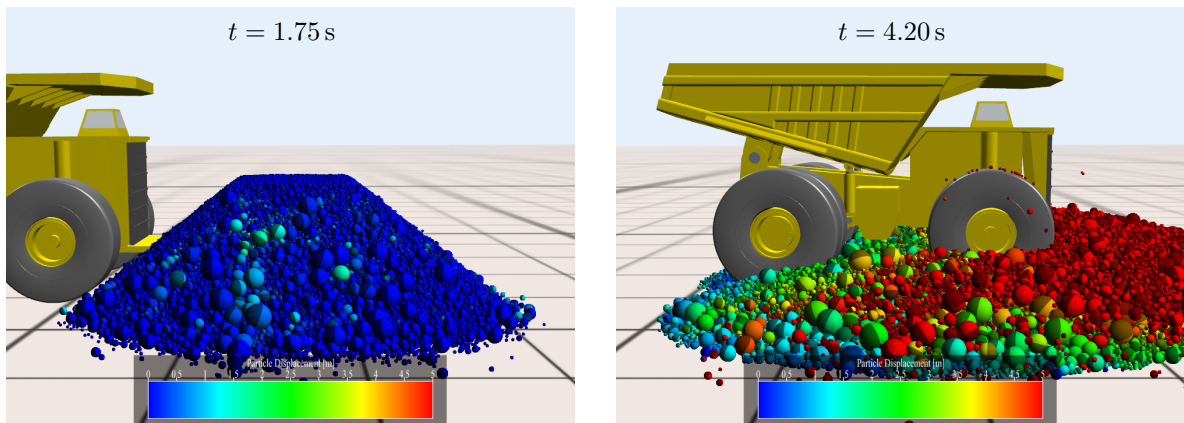


Figure 10: Screenshots of the collision at different time steps t for head-on collision with $v = 40$ km/h and trapezoidal berm with $H = 4$ m and $B = 4$ m.

head-on with a trapezoidal berm. In this case the height is kept constant and the effect of the width of the berm is shown. A more detailed analysis is currently on the way to provide surface mining operators with more rigorous guidelines.

REFERENCES

- [1] Giacomini, A., Thoeni, K.. Full-scale experimental testing of dump-point safety berms in surface mining. *Canadian Geotechnical Journal* (2015) **52**(11):1791–1810.
- [2] Giacomini, A., Thoeni, K.. Energy Adsorption Capacity of Muck Piles and Their Status as Engineered Hard Barriers. Tech. Rep. ACARP C21032, Australian Coal Association Research Program, (2014).
- [3] Alsaleh, M.. Soil – Machine Interaction: Simulation and Testing. In: Bonelli, S., Dascalu, C., Nicot, F., (editors). *Advances in Bifurcation and Degradation in Geomaterials*, Springer Series in Geomechanics and Geoengineering 11. Springer, (2011), p. 165–176.
- [4] Gruening, T., Kunze, G., Katterfeld, A.. Simulating the working process of construction machines. In: Bonelli, S., Dascalu, C., Nicot, F., (editors). *Proceedings of Bulk Solids Europe 2010*. (2010), p. 1–10.
- [5] Kübler, K., Schiehlen, W.. Two methods of simulator coupling. *Mathematical and Computer Modelling of Dynamical Systems* (2000) **6**(2):93–113.
- [6] Algoryx Simulation, . AGX Dynamics. <http://algoryx.se>. (2017).
- [7] Acary, V., Brogliato, B.. *Numerical Methods for Nonsmooth Dynamical Systems: Applications in Mechanics and Electronics*. Springer Verlag, (2008).
- [8] Moreau, J.. Numerical aspects of the sweeping process. *Computer Methods in Applied Mechanics and Engineering* (1999) **177**:329–349.
- [9] Jean, M.. The non-smooth contact dynamics method. *Computer Methods in Applied Mechanics and Engineering* (1999) **177**(3–4):235–257.
- [10] Servin, M., Wang, D., Lacoursière, C., Bodin, K.. Examining the smooth and nonsmooth discrete element approach to granular matter. *International Journal for Numerical Methods in Engineering* (2014) **97**:878–902.
- [11] Servin, M., Wang, D.. Adaptive model reduction for nonsmooth discrete element simulation. *Computational Particle Mechanics* (2016) **3**(1):107–121.
- [12] Lacoursière, C.. Regularized, stabilized, variational methods for multibodies. In: P. Bunus, D.F., Führer, C., (editors). *The 48th Scandinavian Conference on Simulation and Modeling (SIMS 2007), 30-31 October, 2007, Göteborg (Särö), Sweden*,

Linköping Electronic Conference Proceedings. Linköping University Electronic Press, (2007), p. 40–48.

- [13] Murty, K.. *Linear Complementarity, Linear and Nonlinear Programming*. Helderman-Verlag, Heidelberg, (1988).
- [14] Brandl, M.. Agx dynamics two-body tire model - for real-time vehicle simulation. Internal documentation at Algoryx Simulation, (2015).